PUBLISHED BY

INTECH

open science | open minds

World's largest Science, Technology & Medicine Open Access book publisher



2750+
OPEN ACCESS BOOKS



96,000+
INTERNATIONAL AUTHORS AND EDITORS



88+ MILLION
DOWNLOADS



BOOKS
DELIVERED TO 151 COUNTRIES

AUTHORS AMONG
TOP 1%
MOST CITED SCIENTIST



12.2%
AUTHORS AND EDITORS FROM TOP 500 UNIVERSITIES



Selection of our books indexed in the Book Citation Index in Web of Science™ Core Collection (BKCI)

Chapter from the book *Green Chemistry - Environmentally Benign Approaches*
Downloaded from: http://www.intechopen.com/books/green-chemistry-environmentally-benign-approaches

Interested in publishing with InTechOpen?
Contact us at book.department@intechopen.com

4

Electrochemically-Driven and Green Conversion of SO_2 to $NaHSO_4$ in Aqueous Solution

Hong Liu[1,2,*], Chuan Wang[1,2] and Yuan Liu[1]
[1]*Chongqing Institute of Green and Intelligent Technology, Chinese Academy of Sciences, Chongqing,*
[2]*School of Chemistry and Chemical engineering, Sun Yat-sen University, Guangzhou, China*

1. Introduction

The world has widely resorted to fossil fuels to power the industry and everyday life. In China, above 70% of the energy is extracted from coal. Emission of SO_2 due to burning of fossil fuels, in particularly of coal, causes harmful impacts on the environment, human health, livestock, and plants *(1,2)*. Many measures have been taken to cut off the emission of SO_2 during the last generations. It can be seen that the reduction of SO_2 emission in developed countries such as the United States has been witnessed *(3)*. However, due to the aspiration of energy to drive the economic increase and sustain the expanded population, the SO_2 emission is estimated to augment sharply in the rapidly developing Asian areas, and will still pose as a worldwide environmental problem in the next 30 years *(4)*.

Basically, the SO_2 emission is reduced after the burning processes through various flue gas desulfurization (FGD) processes *(5-8)*, which serves to transform the S(IV) to S(VI) and frequently to immobilize the SO_2 waste in the form of a solid. Of them, a wet limestone FGD process *(6,9,10)* using $CaCO_3$ mineral, represents over 90% of the installed desulfurization capacities in the world *(9)*, and can be chemically expressed below :

$$SO_2 + CaCO_3 + 2H_2O + \frac{1}{2}O_2 \rightarrow CaSO_4 \cdot 2H_2O + CO_2 \quad (1)$$

Eq 1 illustrates that the SO_2 is transformed and immobilized in the form of $CaSO_4 \cdot 2H_2O$, which may be commercialized as gypsum, but the incentive is little in areas including the United Sates *(11)* and China because of its rich natural sources. To our knowledge, only 3% of the FGD byproduct gypsum can be reused in China. In fact, once treated improperly, the solid waste becomes a secondary pollutant, and thereby is of a great environmental concern. Meanwhile, eq 1 shows that 1 mole of SO_2 leads to 1 mole of CO_2, whose discharge and

* Corresponding Author

accumulation in the atmosphere is recognized to aggravate a greenhouse effect *(12,13)*. Actually, it is considered that most wet FGD processes have an inherent shortcoming of secondary pollution, or of high running cost if the secondary pollutant is avoided. A challenge to overcome such shortcomings still remains *(14)*.

To meet the challenge, novel green technologies with no/less secondary pollution and with a value-added product become essential. Fan et al. have developed a process of converting the SO_2 to polymeric ferric sulfate, which can be employed as a common coagulant for water and wastewater treatment *(12)*.

Electrochemical techniques, utilizing electrons as a clean reagent, exactly enjoy the sustainability. Since most wet FGD processes embrace a sub-process of electron transfer for the oxidation of S(IV) to S(VI), the electrochemical techniques appear to fitfully work there. The electrochemical cleanup of flue gas has already been tested. For example, SO_2 can be anodically oxidized to H_2SO_4 in aqueous solution *(14-16)*, and regeneration of FGD agents is developed by using electrodialysis with a bipolar membrane *(17,18)*. It should be noted that as air coexists with the SO_2 in flue gas, electrochemical utilization of the molecular oxygen from air to further oxide the SO_2 is indispensable and should be encouraged. Such a new concept, however, has not been implemented so far.

To convert the SO_2 to be a value-added product without secondary pollution, this study aims at developing such a novel and green process by designing a series of electrochemical reactions through a SO_2 absorption-and-conversion process. In the process, a few considerations in the process can benefit the attempt. (i) The cathodic reaction utilizes O_2 from air to scavenge the process-released H^+ ions, while the anodic reaction uses H_2O to supply H^+ ions. (ii) The H^+ scavenging benefits the SO_2 absorption and its further oxidation. (iii) The H^+ supply benefits the formation of a bisulfate. Consequently, the SO_2 conversion is driven electrochemically to form $NaHSO_4$ as a sulfur-containing product.

$NaHSO_4$ is a valuable chemical and widely used as an additive in manufacture of dye stuff, a soil amender in agriculture, and replacement of H_2SO_4 in industry for pH adjustment and catalytic reactions. This study focused on the chemical and sustainable fundamentals as well as the pH optimization for the SO_2 oxidation. The findings are expected to lay a basis of understanding this new design with potential to convert the SO_2 from flue gas to $NaHSO_4$ as a value-added product in a green way.

2. Chemical fundamentals of the process

In this process, the SO_2 is designed to be absorbed into aqueous solution with alkaline, then oxidized to sulfate, and then transformed into bisulfate. The chemical fundamentals should be clarified to understand how the process works.

Absorption of SO_2. In the wet FGD processes, H^+ ions are released upon the absorption of SO_2 into the aqueous solution *(5)*:

$$SO_2 + H_2O \Leftrightarrow H^+ + HSO_3^- \tag{2}$$

$$HSO_3^- \Leftrightarrow H^+ + SO_3^{2-} \tag{3}$$

Oxidation of SO_2 to SO_4^{2-}. After the absorption, the absorbed SO_2 is oxidized by air in aqueous solution at moderate pH from HSO_3^- and SO_3^{2-} to SO_4^{2-} ions. This oxidation process is expressed as follows, of which eq 4 releases H^+ ions, but eq 5 does not *(19)*:

$$HSO_3^- + \frac{1}{2}O_2 \rightarrow SO_4^{2-} + H^+ \tag{4}$$

$$SO_3^{2-} + \frac{1}{2}O_2 \rightarrow SO_4^{2-} \tag{5}$$

ESH. The H^+ ions released through eqs 2~4 need to be scavenged due to their hindrance of the SO_2 absorption. Otherwise, the continuous absorption of SO_2 will be terminated. It can be noted that while O_2 in air is utilized for the SO_2 oxidation through eqs 4 and 5, the cathodic reduction of O_2 can be employed to scavenge the process-released H^+ ions. The reactions of O_2 reduction through a 2-electron process at acidic and neutral/alkaline conditions are expressed in eqs 6 and 6′, respectively *(20-22)*:

$$O_2 + 2H^+ + 2e \rightarrow H_2O_2 \tag{6}$$

$$O_2 + 2H_2O + 2e \rightarrow H_2O_2 + 2OH^- \tag{6'}$$

At the same time, a side reaction co-exists with eq 6 below:

$$2H^+ + 2e \rightarrow H_2 \uparrow \tag{7}$$

It can be seen that eqs 6 and 7 consume H^+ ions and eq 6′ supplies OH^- ions. All these reactions can be utilized to scavenge the H^+ ions released through eqs 2~4.

Transformation of SO_4^{2-} to Bisulfate. As coupled to the cathodic reactions, an anodic reaction is shown below:

$$H_2O \rightarrow \frac{1}{2}O_2 \uparrow + 2H^+ + 2e \tag{8}$$

Under an extremely acidic condition, the H^+ ions in eq 8 are combined with the SO_4^{2-} ions formed in eqs 4 and 5 to form a bisulfate:

$$SO_4^{2-} + H^+ \Leftrightarrow bisulfate\ ion \tag{9}$$

As a result, a model experiment becomes necessary to chemically substantiate this design by disclosing the ESH effect on the SO_2 absorption and oxidation, and by confirming the formation of $NaHSO_4$ as a product of desulfurization.

3. Experimental section

Chemicals and Reagents. SO_2 gas (99.9%) was obtained from KEDI, Foshan, China. Other chemicals as analytical reagents were used as obtained. Double distilled water was used in all experiments.

Experimental Procedure. The model experiment to substantiate this design was performed in an experimental setup as schemed in Figure 1, which consists of two 200 mL chambers: a DS chamber with a graphite rod (ø = 6.4 mm, and L = 200 mm, Chenhua, Shanghai, China) as the cathode and a saturated calomel electrode as the reference electrode, and an SR chamber with a Pt flake (2 × 1.5 cm^2, Chenhua, Shanghai, China) as the anode. Both chambers were connected by a salt bridge containing saturated Na_2SO_4 solution with agar. A PS-1 potentiostat/galvanostat (Zhongfu, Beijing, China) was employed to apply a cathodic current. The solution temperature was kept by a water bath at 25.0 ± 0.5 °C and monitored by a thermometer. Air was purged onto the cathode surface by an air pump through a glass frit diffuser, and a needle valve was used to control its flow rate.

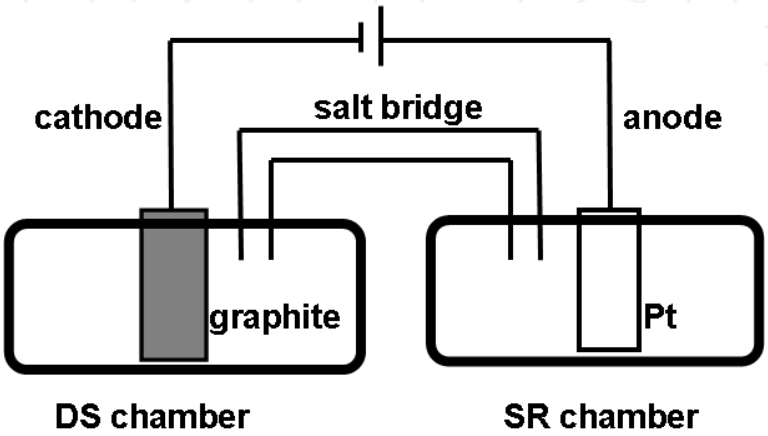


Fig. 1. Scheme of the experimental setup: DS chamber is desulfurization chamber, and SR chamber is sulfur-recovery chamber.

To quantify the OH^- ions electrochemically generated in the DS chamber and the H^+ ions in the SR chamber, electrochemical reactions of eqs 6, 6′, 7 and 8 were performed in 0.01 M Na_2SO_4 solution without SO_2 at pH_0 6.0, in which an air flow of 100 mL min^{-1} and different current densities of 0.10, 0.15, 0.20, 0.25, and 0.30 mA cm^{-2} were applied. During the reactions, 0.01 M HCl and 0.01 M NaOH solutions were fed by a pump (Longer BTOQ-50M, Baoding, China) into the DS chamber and SR chamber, respectively, to maintain the pH at 6.0 ± 0.2. At the same time, 1.0 mL of solution sample was taken from the DS chamber for the quantification of H_2O_2 generation.

After that, two steps of the model experiment were performed in a batch mode. Step I was performed in the DS chamber, and Step II, in the SR chamber. Each experiment was performed three times and the values of experimental data in average are presented.

Prior to Step I, a start-up procedure was carried out to pre-store OH^- ions in the DS chamber through eqs 6′, and thus a solution $pH_0 \geq 9.0$ in this chamber was obtained. The start-up procedure was described below, which was performed in the setup as schemed in Figure 1. Upon application of a cathodic current density as large as 0.60 mA cm^{-1} to preclude the generation of cathodic byproduct H_2O_2 *(20)*, air with 100 mL min^{-1} flow rate was bubbled into water in the DS chamber to allow eq 6′ to occur. The coupled reaction of eq 8 occurred

simultaneously in the SR chamber. This start-up procedure continued till the pH increase to ≥ 9.0 in the DS chamber. Then, the solution in the SR chamber was discarded, and the solution in the DS chamber containing the pre-stored OH^- ions was utilized to absorb the SO_2 gas in Step I of the model experiment.

Thereafter, the SO_2 absorption of Step I was performed without current application. Initially, nitrogen gas was bubbled into the solution to remove any oxygen, then gaseous SO_2 was introduced into the alkaline solution to form A-SO_2 till pH decreased below 7.0.

In the A-SO_2 oxidation of Step I, an air flow at 100 mL min^{-1} was purged onto the cathode placed in the A-SO_2 solution. And a cathodic current was applied to maintain the electrochemical reactions. The A-SO_2 oxidation proceeded till the solution pH recovered to neutral pH (7.0).

To optimize the pH for the A-SO_2 oxidation, a set of experiments was performed at 1.0 mM A-SO_2 concentration, and different pHs in the range of 4.0~8.0 were maintained by chemical dosing of 0.01 M NaOH solution except at pH_0 8.0.

In the transformation of SO_4^{2-} to bisulfate of Step II, the reacted solution of Step I was relocated from the DS chamber to the SR chamber. Step II proceeded under a cathodic current with solution pH decrease in the SR chamber, while it stopped upon that the pH in the DS chamber reached the pH_0 value at the start-up step.

In Step I, the A-SO_2 concentrations were monitored by taking 1.0 mL of solution samples at pre-set time intervals, and 5 μL of methanol was injected into the samples taken during the A-SO_2 oxidation to quench any possible radical reaction (*23)*. After Step I, SO_4^{2-} concentrations were measured. After Step II, H^+, Na^+, and SO_4^{2-} concentrations were measured.

Notably, in actual wet FGD processes, the SO_2 absorption and oxidation in Step I occur concurrently. However, to understand the ESH effect on the SO_2 absorption and its oxidation independently, the two experiments were conducted separately. At the same time, the air content in actual FGD processes should be minimized, and thus a small rate of 100 mL min^{-1} was fixed without further optimization. It was believed that an alkaline condition at pH > 7.0 was beneficial to the SO_2 absorption, and an acidic condition at pH < 3.0 was beneficial to the $NaHSO_4$ formation, while the A-SO_2 oxidation relied on pH, so the pH optimization for the A-SO_2 oxidation was performed.

Chemical Analysis. Measurement of the concentrations of electrochemically-generated OH^- and H^+ ions is accomplished by counting the dose of added H^+ solution with a known concentration to determine the amount of OH^-, and by counting that of OH^- to determine that of H^+. The A-SO_2 concentration was determined in terms of S(IV) concentration using a UV-VIS spectrosphotometer (TU1810, Universal Analysis, Beijing, China) according to a reported procedure *(24)*. The H_2O_2 concentration was determined by spectrophotometry according to a potassium titanium (IV) oxalate method *(20)*. The SO_4^{2-} and Na^+ concentrations were measured by ion chromatography (Dionex DX-600, U.S.). The cyclic voltammetry of A-SO_2 solution was performed in a N_2-saturated solution with 0.05 mM Na_2SO_4 as electrolyte on a CHI work station (Chenhua, Shanghai, China) with 50 mV s^{-1} scanning rate. The pH was monitored by a pH meter (PB-10, Sartorius, Shanghai, China).

4. Results and discussion

Electrochemical Generation of OH^- and H^+ Ions. This designed process underlined (i) that the electrochemical scavenging of process-released H^+ ions due to eqs 2~4 would benefit the SO_2 absorption and oxidation, and (ii) that the electrochemical supply of H^+ ions through eq 8 would realize the $NaHSO_4$ formation. Three cathodic reactions of eqs 6, 6′, and 7 served to increase the solution pH and electrochemical generation of OH^- ions should be considered. Figure 2A illustrated that the OH^- concentration in the DS chamber increased proportionally to the reaction time and the accumulative rate of OH^- ions depended on the applied current density. In the meantime, H_2O_2 was generated through eq 6 and 6′. Figure 1B revealed that the H_2O_2 concentration increased against the reaction time. As paired to the cathodic reactions, anodic reaction of eq 8 occurred to supply H^+ ions in the SR chamber. Measurements of the H^+ ions revealed that the H^+ concentration increased at the same rate as that of OH^- ions in the DS chamber (not shown here).

The electrochemically-generated OH^- ions in the DS chamber and H^+ ions in the SR chamber carried electrons, which must be balanced electrically to keep the electrical neutralization of solution in each chamber. An analysis of electron balance will be described later.

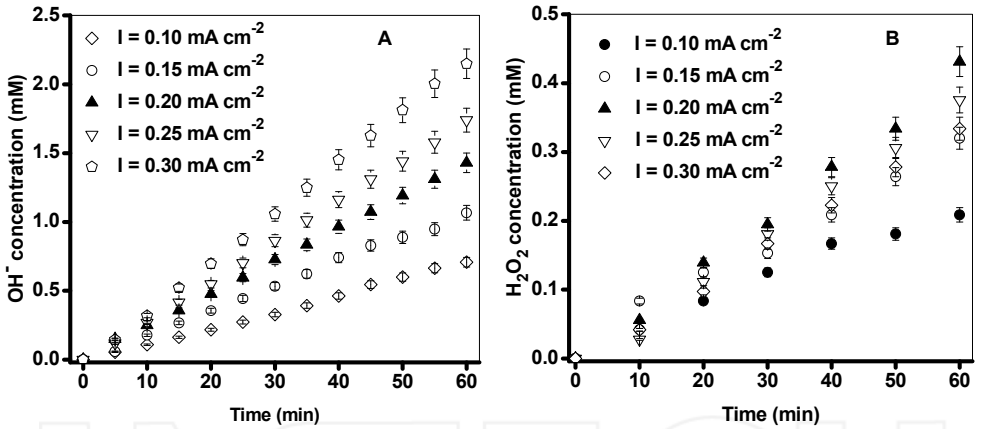


Fig. 2. Buildup of electrochemically-generated OH^- ions (A), and H_2O_2 (B) in the DS chamber.

ESH Effect on SO_2 Absorption. The above electrochemically-generated OH^- ions could be utilized to scavenge the absorption-released H^+ ions through eqs 2 and 3. ESH has two functions. One was the pre-storage of OH^- ions through eq 6′, which later served to scavenge the SO_2-absorption-released H^+ ions. The other was the *in situ* scavenging of the process-released H^+ ions through eqs 6 and 7 or *in situ* supplying OH^- ions through eq 6′, which also served to scavenge the A-SO_2-oxidation-released H^+ ions.

To disclose the ESH effect on the SO_2 absorption, one SO_2 absorption experiment in Step I of the model experiment was performed at pH_0 9.0 with pre-stored OH^- ions, and then two additional SO_2 absorption experiments without pre-stored OH^- ions were performed at pH_0 5.0 and 7.0, respectively. Figure 3 revealed that under the three pH conditions, the A-SO_2

increased first quickly, then slowly to a plateau. Comparatively, at pH_0 9.0, the A-SO_2 concentration increased most rapidly and ended at the highest level. The acceleration of SO_2 absorption at pH_0 9.0 was caused by the lifted pH, which was realized by pre-storing the OH^- ions electrochemically. Obviously, the pre-stored OH^- ions served to scavenge the SO_2-absorption-released H^+ ions as a means of ESH. Thus, the SO_2 absorption was accelerated by the ESH.

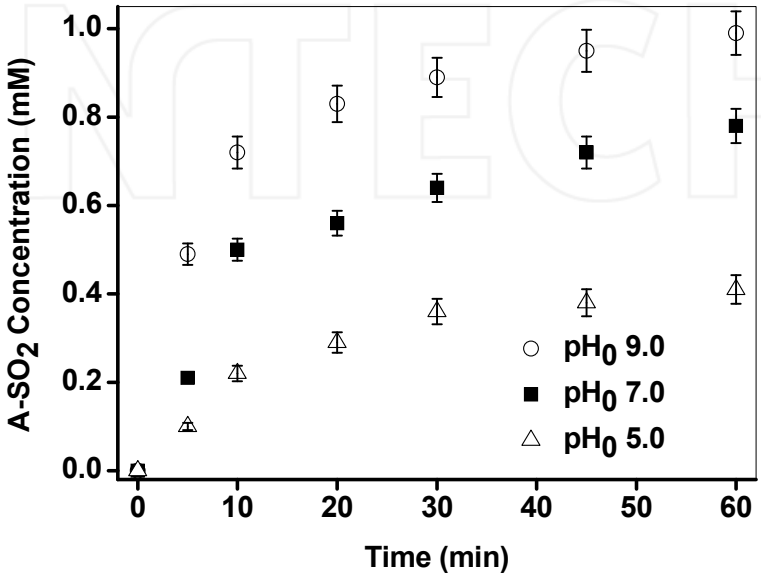


Fig. 3. Buildup of A-SO_2 concentration in the SO_2 absorption at solution pH_0 5.0, 7.0, and 9.0.

ESH Effect on A-SO_2 Oxidation. The oxidation-released H^+ ions were in situ scavenged through eqs 6, 6′ or 7. To disclose the ESH effect on the A-SO_2 oxidation, two sets of SO_2 oxidation experiments in Step I were carried out. In the first set with ESH, a current density at 0.20 mA cm^{-2} was applied to maintain the electrochemical reactions, while in the second set without SH, no current density was applied.

Figure 4 showed that with ESH, 100% and 95.8% of A-SO_2 disappearances were achieved at 30 min for the 1.0 mM A-SO_2 and 1.5 mM A-SO_2 solutions, respectively. Following the oxidation reaction, SO_4^{2-} concentrations were detected, and the results as listed in Table 1 indicated that 95.0% and 88.0% of the A-SO_2 were converted to SO_4^{2-} ions. By contrast without SH, only 70.7% of the 1.0 mM A-SO_2 and 60.9% of the 1.5 mM A-SO_2 disappeared after 30 min, and the SO_4^{2-} concentrations in the reacted solution were significantly lower than those with ESH (Table 1). From these it could be understood that the A-SO_2 oxidation with ESH proceeded more rapidly than that without SH, since ESH was beneficial to the conversion of A-SO_2 oxidation to SO_4^{2-}.

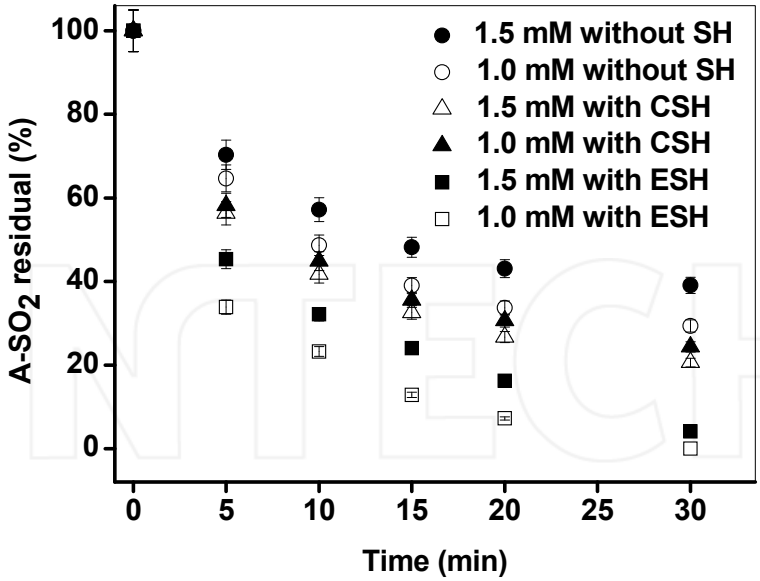


Fig. 4. Temporal disappearance of A-SO_2 concentration in the A-SO_2 oxidation at pH_0 6.0, with ESH at 0.20 mA cm^{-2} current density for 1.0 mM A-SO_2 and 0.25 mA cm^{-2} current density for 1.5 mM A-SO_2, with CSH, and without SH.

A-SO_2 (mM)	SO_4^{2-} with ESH (mM)	SO_4^{2-} with CSH (mM)	SO_4^{2-} without SH (mM)
1.0	0.98	0.78	0.66
1.5	1.32	1.15	0.97

Table 1. SO_4^{2-} concentrations after the A-SO_2 oxidation at pH_0 6.0, with ESH at 0.20 mA cm^{-2} current density for 1.0 mM A-SO_2 and 0.25 mA cm^{-2} current density for 1.5 mM A-SO_2, with CSH, and without SH.

To further disclose the ESH effect, a set of experiments in 1.0 mM and 1.5 mM A-SO_2 solutions was carried out with CSH, and the results are added in Figure 4. Clearly, the A-SO_2 oxidations with CSH proceeded more rapidly than those without SH, but more slowly than those with ESH. Therefore, it was further confirmed that the SH benefited the A-SO_2 oxidation, while the ESH was more effective than the CSH.

Moreover, the results in Table 1 showed that more SO_4^{2-} ions were obtained in the reacted solution with ESH than those with CSH. It was believed that the H_2O_2 produced through eq 6 or 6′ could enhance the SO_2 oxidation as an oxidizing reagent *(27,28)*. After the reaction, no H_2O_2 residue left as impurity in the final sulfur-containing product. Therefore, the ESH benefited the A-SO_2 oxidation with two advantages of (i) scavenging the absorption- and oxidation-released H^+ ions, and (ii) simultaneously generating H_2O_2 to facilitate the conversion of A-SO_2 to SO_4^{2-}.

Transformation of Na_2SO_4 to $NaHSO_4$. Beyond the utilization of cathodic reaction to scavenge the H^+ ions released in eqs 2~4, this new process utilized an anodic reaction (eq 8) to supply H^+ ions which combined the SO_4^{2-} to form bisulfate. In both Steps I and II, the H^+ ions were produced in the SR chamber. Step II was performed by relocating the reacted solution of Step I from the DS chamber to the SR chamber where eq 8 occurred. Thus after this step, three ions of Na^+, H^+, and SO_4^{2-} presented in the SR chamber, and the analysis of mass balance of electrons as would be shown later suggested that a mixture of the three ions might result in the formation of $NaHSO_4$ through eq 9.

To confirm the $NaHSO_4$ formation, after the two-step model experiments with 1.0 mM and 1.5 mM A-SO_2 concentrations, the concentrations of the three ions in the SR chamber were measured. The results as shown in Figure 5 demonstrated that a mass balance of Na^+, H^+ and SO_4^{2-} ions was approximately 1:1:1, which ensured the $NaHSO_4$ formation.

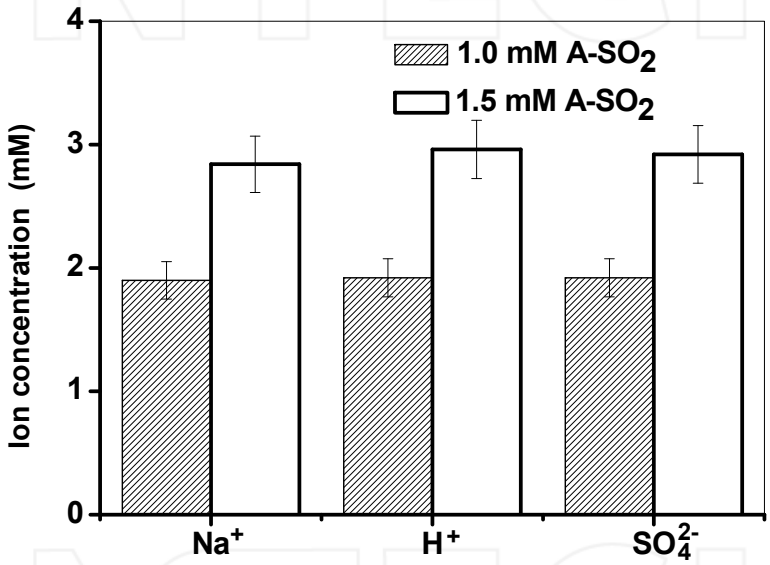


Fig. 5. Ion concentrations measured in the SR chamber after the model experiment.

Optimization of pH for A-SO_2 Oxidation with ESH. Figure 6A demonstrated that pH 5.0~6.0 was optimal for the A-SO_2 oxidation, which was in good agreement with others' results of optimal pH 6.0 kept by addition of OH^- ions in the SO_2 oxidation by air during a seawater FGD process *(24)*. Figure 6B showed the records of cyclic voltammetry in A-SO_2 solution, which confirmed that the optimal pH for the SO_2 oxidation was 5.0~6.0.

Figure 6B illustrates the cyclic voltammetry recorded in the 1.0 mM A-SO_2 solution, and the peaks at 0.12~0.15 V and 0.81~0.83 V were associated with the HSO_3^- oxidation and the SO_3^{2-} oxidation, respectively. On the other hand, the A-SO_2 solution consists of two major species of HSO_3^- and SO_3^{2-} in the pH range of 4.0~9.5. It has been documented that the HSO_3^- species occupies 100%, 92%, 38% and 10% of A-SO_2 at pH_0 5.0, 6.0, 7.0 and 8.0, respectively *(27)*.

Clearly, the peaks associated with the HSO_3^- oxidation were not pronounced at pH 7.0 and 8.0, while the peaks were mature at pH 5.0 and 6.0. On the contrary, the peaks associated with the SO_3^{2-} oxidation were mature at pH 7.0 and 8.0, while no peak was observed at 5.0 and 6.0 since the SO_3^{2-} species were only 8% and 0, respectively. These results implied that at optimal pH 5.0~6.0, the HSO_3^- predominated in the A-SO_2. Moreover, the HSO_3^- oxidation proceeded more rapidly at this pH range than at pHs beyond this range. Thus, the optimal pH for the A-SO_2 oxidation was pH 5.0~6.0.

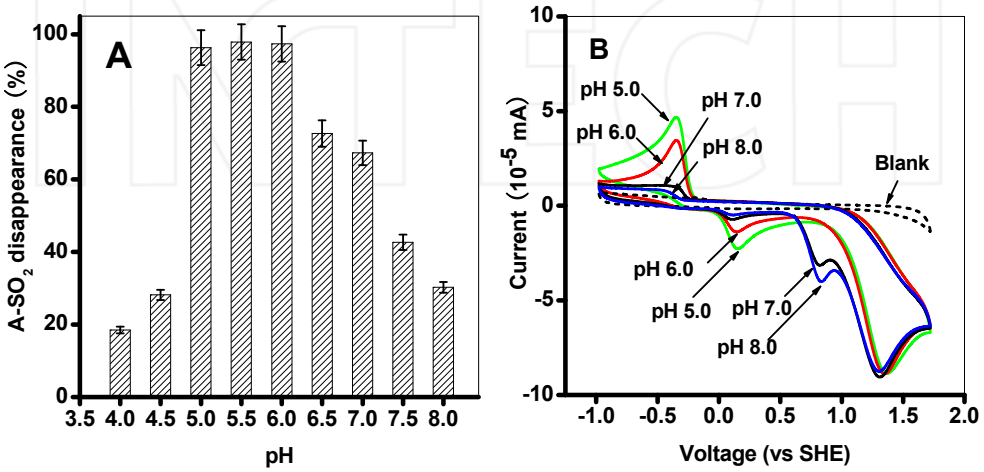


Fig. 6. Dependence of 1.0 mM A-SO_2 disappearance after 30 min oxidation on the solution pH (A), and cyclic voltammetry recorded in 1.0 mM A-SO_2 solution (B).

In real application, the current density should be adjusted to maintain the optimal range of pH 5.0~6.0 for the A-SO_2 oxidation. Consequently, a set of 1.0 mM A-SO_2 oxidation experiments was performed at pH_0 5.0, 6.0, 7.0, and 8.0. It was found that when the current densities were adjusted to 0.20, 0.25, and 0.30 mA cm^{-2}, the optimal pH 5.0~6.0 could be maintained for pH_0 7.0, 6.0, and 5.0, respectively. Evidently, the current density to maintain the optimal pH increased with the pH_0 decrease of A-SO_2 solution. The lower pH_0 meant more H^+ ions in the solution, so the higher current density was required to scavenge the H^+ ions. At pH_0 8.0, the SO_3^{2-} species predominated in the A-SO_2 solution *(27)*, and no pH decrease was observed in the A-SO_2 oxidation by air as indicated by eq 5. Thus no application of cathodic current to generate OH^- ions was required.

Analysis of Electron Balance in DS Chamber and SR Chamber. In this study, OH^- ions were generated through eq 6′ in the DS chamber, and H^+ ions were generated through eq 8 in the SR chamber. The electrons carried by the OH^-, H^+, and other emerged ions must be balanced electrically to keep the electrical neutralization of solution in either chamber. Table 2 lists the ion species after each step in the DS chamber and SR chamber. From the ion species, the analysis of electron balance could be made.

	DS chamber	SR chamber
Step I	HSO_3^- Na^+ (pre-stored) SO_4^{2-} from eq 4 Na^+ from salt bridge OH^- from eq 6′	H^+ from eq 8 SO_4^{2-} from salt bridge
Step II	OH^- from eq 6′ Na^+ from salt bridge ----	H^+ and SO_4^{2-} coming from Step I Na^+ and SO_4^{2-} relocated from DS chamber of Step I, H^+ from eq 8 SO_4^{2-} from salt bridge

Table 2. Ion species after each step in the DS chamber and SR chamber.

In the DS chamber, Step I, the absorption-released H^+ ions through eqs 2 and 3 were scavenged by the pre-stored OH^- ions. After Step I, HSO_3^- ions predominated in the A-SO_2 solution at pH 5.0~6.0 *(27)*. Clearly, the HSO_3^- ions were electrically balanced by the pre-stored Na^+ ions.

In the DS chamber, Step I, the oxidation-released H^+ ions through eq 4 were scavenged by the OH^- ions that were in situ generated through eq 6, 6′, or 7. The A-SO_2 oxidation through eq 4 generated SO_4^{2-} ions as product of Step I. Concurrently, Na^+ ions were released from the salt bridge to balance the SO_4^{2-} ions electrically. In the SR chamber, Step I, accompanied generation of H^+ ions occurred through eq 8. The H^+ ions were balanced electrically by the SO_4^{2-} ions released from the salt bridge (Figure 1).

In the SR chamber, Step II, the H^+ and SO_4^{2-} ions from Step I that were electrically balanced mutually from Step I stayed there. And the mutually balanced Na^+ and SO_4^{2-} ions from Step I were relocated to this chamber. At the same time, H^+ ions continued to be generated through eq 8. Accordingly, SO_4^{2-} ions continued to release from the salt bridge to balance the H^+ ions. Therefore, the electron balance resulted in a mixture of H_2SO_4 and Na_2SO_4 in the SR chamber after Step II. Since a reaction of Na_2SO_4 and H_2SO_4 is often adopted to manufacture $NaHSO_4$ in industry, $NaHSO_4$ might be obtained as a product in the SR chamber after Step II.

Additionally in the DS chamber, Step II, accompanied generation of OH^- ions occurred through eq 6′. The OH^- ions were balanced electrically by the Na^+ released from the salt bridge (see Figure 1).

Process of Electrochemically-driven Conversion of SO_2 to $NaHSO_4$. Up to now, this process design has been chemically substantiated, and the oxidation reaction of A-SO_2 can be optimized. Accordingly, a process of the SO_2 conversion to $NaHSO_4$ was schemed in Figure 5 to show the mass flows of SO_2, OH^- and H^+ ions, while those of Na^+ and SO_4^{2-} ions are presented in Figure 8. Figures 7 and 8 illustrate that the SO_2 gas is converted to $NaHSO_4$ through two stages: (i) SO_2 absorption plus oxidation to Na_2SO_4 in the DS chamber, and (ii) transformation of Na_2SO_4 to $NaHSO_4$ in the SR chamber.

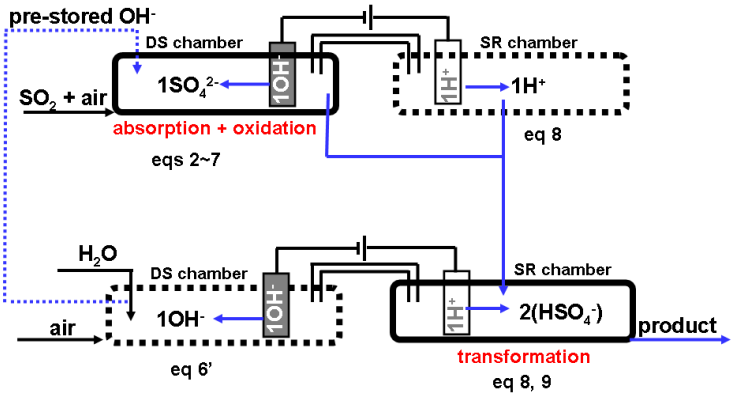


Fig. 7. Mass flow of SO_2, OH^-, and H^+ ions in the process of SO_2 conversion to $NaHSO_4$ in aqueous solution: the number before the species designates their mole mass.

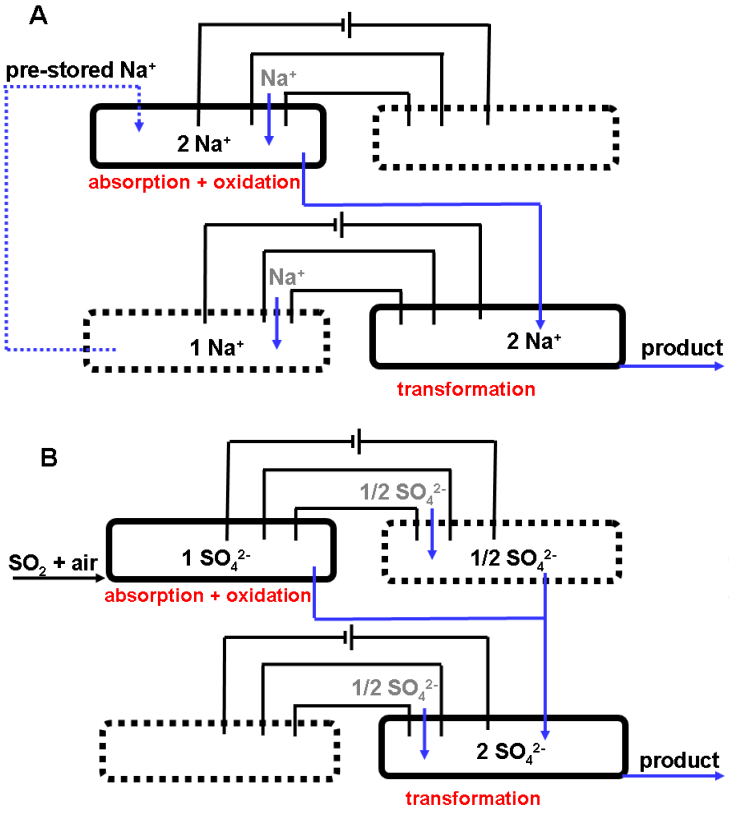


Fig. 8. Mass flow of Na^+ (A) and SO_4^{2-} (B) ions in the proposed process of SO_2 conversion to $NaHSO_4$ in aqueous solution: the number before the species designates their mole mass; chambers in left hand are DS chamber, and in right hand, SR chamber.

Figure 7 illustrates that in the first stage, the SO_2 gas with the co-existing air is introduced into the aqueous solution where the reactions through eqs 2~7 occur to form Na_2SO_4. The SO_2 absorption occurs effectively at high pH, and the A-SO_2 oxidation occurs rapidly at pH 5.0~6.0 but quite slowly at pH 8.0. Thus, although occurring concurrently, the SO_2 absorption predominates first at pH above 6.0, and then the A-SO_2 oxidation becomes the main reaction at pH 5.0~6.0. In the second stage, the solution containing Na_2SO_4 is relocated from the DS chamber to the SR chamber, and then the Na_2SO_4 is transformed into $NaHSO_4$ (eq 9) under an acidic condition through eq 8.

Accompanied with the A-SO_2 oxidation in the DS chamber, H^+ ions are generated (eq 8) in the SR chamber for the subsequent formation of $NaHSO_4$. Accompanied with the $NaHSO_4$ transformation in the SR chamber, OH^- ions are generated (eq 6′) in the DS chamber and pre-stored for the operation of next run.

To practice this new process, some findings from this study may be summarized as tips: (i) alkaline condition at pH > 7.0 in the DS chamber is beneficial to the SO_2 absorption, which can be achieved by the electrochemical pre-storage of OH^- ions through eq 6′, (ii) electrochemical generation of H_2O_2 (eqs 6 and 6′) in the DS chamber can be designed as a concurrent reaction with the A-SO_2 oxidation reaction by air, since the H_2O_2 can accelerate the A-SO_2 oxidation reaction significantly, and (iii) a suitable current density shall be adjusted to maintain the optimal pH 5.0~6.0 of the A-SO_2 oxidation reaction.

Thus by combination of the mass flow in Figure 8, an overall reaction can be expressed below to illustrate the SO_2 conversion into $NaHSO_4$ under the electrical driving force:

$$SO_2 + \frac{1}{2}O_2 + H_2O + Na_2SO_4 \xrightarrow{electricity} 2NaHSO_4 \tag{10}$$

Eq 10 indicates that from a thermodynamic point of view, the electrochemical reactions of eqs 6, 6′, 7 and 8 may not be essential, but from an engineering point of view, they are critical. The cathodic reactions scavenge the absorption- and oxidation-released H^+ ions to drive the SO_2 absorption and oxidation, and the anodic reaction provides H^+ ions to drive the $NaHSO_4$ formation. Therefore, the electrochemical reactions ensure the process of SO_2 conversion to $NaHSO_4$ through eq 10.

Sustainability Evaluation of The Process. Green chemistry has a set of principles to minimize pollution as far as possible in chemical processes, including achieving high value of atom economy in the synthetic process, eliminating toxicity to human health and the environment, minimizing energy consumption, utilizing clean materials, and so on *(28,29)*. Although the aspiration of green chemistry is preferably realized in the manufacturing processes rather than the subsequent cleanup of effluent, the principles are still applicable in the wet FGD process. In this study, sustainability of this new process was evaluated from the perspective of green chemistry.

The atom economy is expressed by *AU*, which is defined by a ratio of mole mass between the desired product and the reactant(s) as shown below:

$$AU = \frac{mole\ mass\ in\ desired\ product}{mole\ mass\ in\ reac\tan t(s)} \times 100\% \tag{11}$$

The *AU* values of eqs 1~10 are listed in Table 3. Clearly, eqs 5, 6, 9, and 10 received 100% of *AU*. Eqs 2, 3, and 4 received *AU* as high as 98.8%, 98.8%, and 90.0%, respectively. Only eqs 7 and 8 received 50.0% and 11.1%, respectively.

eq	*AU* (%)	desired product	byproduct
1	75.5	$CaSO_4 \cdot 2H_2O$	CO_2
2	98.8	HSO_3^-	H^+
3	98.8	SO_3^-	H^+
4	90.0	SO_4^{2-}	H^+
5	100	SO_4^{2-}	no
6	100	H_2O_2	no
7	50.0	OH^-	H_2O_2
6′	----	no	H_2
8	11.1	H^+	O_2
9	100	bisulfate	no
10	100	$NaHSO_4$	no

Table 3. Values of Atom Utilization (*AU*), desired products, and byproducts in eqs 1~10.

In addition to the individual *AU* values of single reaction, the byproducts of eqs 1~10 are listed in Table 3, and their fates and environmental impacts are discussed as follows. The H^+ ions as byproduct in eqs 2~4 are scavenged to form H_2O, and the H_2O can be reused through eq 8 to generate H^+ ions that entirely end up in the $NaHSO_4$ through eq 9. The H_2O_2 in eq 6 or 6′ is reused to enhance the A-SO_2 oxidation and also enters into the $NaHSO_4$. The gaseous byproducts of H_2 in eq 6′ and O_2 in eq 8 escape into the environment, whereas it is not hazardous to human health and the environment, while some safety measure should be taken to deal with the H_2. However, all other atoms are kept in the final product through reusing the byproducts in the same setup.

Therefore, it can be seen that except the portion of oxygen and hydrogen atoms that released as gases through eqs 7 and 8, respectively, all other atoms are remained in the final product. This process in essence utilizes the raw materials of Na_2SO_4, O_2 in ambient air, and water which are all environmentally clean. As a result, secondary pollution can be avoided.

The electricity consumption (*E*) in terms of kWh through eqs 6, 6′, 7 and 8 is calculated in light of the two-step model experiment.

In the A-SO_2 oxidation of Step I, electricity was consumed through the cathodic reactions of eqs 6, 6′, and 7 to scavenge the H^+ irons released in eqs 2~4, and its consumption was calculated by:

$$E = \frac{\bar{U} \cdot I \cdot t \cdot 10^{-3}}{64 \cdot (C_0 - C_t) \cdot 10^{-3} \cdot S} \tag{S1}$$

where $\bar{U}$ and *I* were the voltage in average and current that kept constant, respectively, the C_0 and C_t were the A-SO_2 concentrations before and after the oxidation reaction, respectively, and *S* was the volume.

In this study, C_0 = 1.0 × 10^{-3} M, C_t = 0.02 10^{-3} M, I = 8.0 × 10^{-3} A, $\bar{U}$ = 4.0 V, t = 0.5 h, and S = 0.20 L; C_0 = 1.5 × 10^{-3} M, C_t = 0.18 10^{-3} M, I = 10.0 × 10^{-3} A, U = 4.3 V, t = 0.5 h, and S = 0.20 L. Thus, in both cases, 1.28 kWh of electricity was consumed in the oxidative conversion of every kg of A-SO_2 to Na_2SO_4 in Step I.

Experimental results showed that the H^+ ions scavenged by eqs 6, 6′, and 7 in the A-SO_2 oxidation of Step I were equivalent to the H^+ ions electrochemically generated through eq 8 in Step II. Thus, the E values of the A-SO_2 oxidation and Step II were equal, and doubled electricity of A-SO_2 oxidation, i.e. 2.56 kWh was consumed to convert every of kg A-SO_2 to $NaHSO_4$.

Figure 7 demonstrates that the OH^- ions were pre-stored through eq 6′ in Step II. Obviously, the electricity consumption to pre-store the OH^- ions for Step I was included in Step II. Therefore, a total electricity of 2.56 kWh was needed for the overall conversion of every kg of gaseous SO_2 to $NaHSO_4$ in aqueous solution, which was only slightly higher than the electricity consumption between 1.8 and 2.4 kWh for the anodic oxidation conversion of one kg of SO_2 into H_2SO_4 in aqueous solution *(14)*. In comparison, the electricity consumption by the electrochemical reactions of this new process seems quite competitive.

Also important, the final product of $NaHSO_4$ has an added value. Eq 10 indicates that 2.06 kg of Na_2SO_4 needs to be consumed to convert one kg of SO_2 to attain 3.75 kg of $NaHSO_4$ with 82% increase in mass. It is learned from the current market that $NaHSO_4$ has an approximately quadruple commercial value of Na_2SO_4. In addition, the alkaline and acid demanded by this new process are provided on site electrochemically instead of addition of chemicals. Considering that the alkaline and acid are manufactured at the price of electricity, we can presume that this approach appears clean and cheap.

Therefore, this new process can fully comply with the principles of green chemistry and shows promising feasibility. If it is flexibly applied in a wet FGD process for SO_2 removal, it could be an environmentally-sustainable technique. In fact, few of environmental processes, which serve to decompose the pollutants, have high value of atom economy. Fortunately, all the atoms from the raw materials in this process end up in the product of $NaHSO_4$. During the process, some intermediates are involved, while they are reusable and environmentally benign.

Further Investigations. Before this process is practiced for reduction of SO_2 in flue gas, more investigations remain. First, effect of CO_2 which abounds in the flue gas should be precluded. We will demonstrate elsewhere that the CO_2 can be separated advisably from the SO_2 in this process, and then the CO_2 can be further captured and recovered electrochemically in the manner of synchronous supply of alkaline and acid. Second, a side reaction that accompanies the cathodic reaction of O_2 reduction is the H_2 evolution (eq 7). A coupling of this reaction with the anodic oxidation of H_2O (eq 8) shows the well-know reaction of H_2O electrolysis. While eq 7 also outputs OH^-, the reaction of H_2O electrolysis consumes extra energy. Thus, the H_2O electrolysis must be avoided by a careful operation of the electrochemical reactor and selection of cathode on which the H_2 evolution can be inhibited. Third, eq 6 has a byproduct of H_2O_2, which serves to accelerate the S(IV) oxidation. Under some circumstances such as on Pt modified carbon electrode, the O_2 reduction proceeded in a 4-electron pathway to solely output OH^- free of H_2O_2. In this case,

the S(IV) oxidation is accomplished by the air oxidation while the overall reaction of $NaHSO_4$ production remains. Since the air oxidation of S(IV) is fast to some extent, and thus in practice, whether the H_2O_2 is essential needs further scrutiny. Forth, a salt bridge is employed in this study to spatially separate the cathodic and anodic chambers. In real application, a membrane *(17,18)* that is commercially available can be employed. Anyway, this new process is promising as an alternative FGD process that immobilizes the SO_2 waste in the form of non-calcium product by means of a cheap and non-toxic material, and thereby avoids the concern over any secondary pollution *(30)*.

5. Nomenclature

A-SO_2 = absorbed SO_2 in aqueous solution
AU = atom utilization in %
CSH = chemical scavenging of H^+ ions through addition of NaOH solution
DS = desulfurization chamber, as cathodic chamber
ESH = electrochemical scavenging of H^+ ions through eqs 6, 6′ or 7
FGD = flue gas desulfurization
SH = scavenging of H^+ ions
SR = sulfur-recovery chamber, as anodic chamber

6. Acknowledgements

This work was supported by Natural Science Foundation of China (Project No: 50978260, 21077136).

7. References

[1] Philip, L.; Deshusses, M. A. Sulfur dioxide treatment from flue gases using a biotrickling filter-bioreactor system. *Environ. Sci. Technol.* 2003, *37*, 1978-1982.
[2] Srivastava, R. K.; Jozewicz, W. Flue gas desulfurization: the state of the art. *J. Air Waste Manage. Assoc.* 2001, *51*, 1676-1688.
[3] Lynch, J. A.; Bowersox, V. C.; Grimm, J. W. Acid rain reduced in eastern United States. *Environ. Sci. Technol.* 2000, *34*, 940-949.
[4] Cofala, J.; Amann, M.; Gyarfas, F.; Schoepp, W.; Boudri, J. C.; Hordijk, L.; Kroeze, C.; Li, J.; Lin, D.; Panwar, T. S.; Gupta, S. Cost-effective control of SO_2 emissions in Asia. *J. Environ. Manage.* 2004, *72*, 149-161.
[5] Kikkawa, H.; Nakamoto, T.; Morishita, M.; Yamada, K. New wet FGD process using granular limestone. *Ind. Eng. Chem. Res.* 2002, *41*, 3028-3036.
[6] Gutiérrez Ortiz, F. J.; Vidal, F.; Ollero, P.; Salvador, L.; Cortés, V.; Giménez, A. Pilot-plant technical assessment of wet flue gas desulfurization using limestone. *Ind. Eng. Chem. Res.* 2006, *45*, 1466-1477.
[7] Karatza, D.; Prisciandaro, M.; Lancia, A.; Musmarra, D. Calcium bisulfite oxidation in the flue gas desulfurization process catalyzed by iron and manganese ions. *Ind. Eng. Chem. Res.* 2004, *43*, 4876-4882.
[8] Lancia, A.; Musmarra, D. Calcium bisulfite oxidation rate in the wet limestone-gypsum flue gas desulfurization process. *Environ. Sci. Technol.* 1999, *33*, 1931-1935.

[9] Hrastel, I.; Gerbec, M; Stergaršek, A. Technology optimization of wet flue gas desulfurization process. *Chem. Eng. Technol.* 2007, *30*, 220-233.
[10] Michalski, J. A. Equilibria in limestone-based FGD process: magnesium addition. *Ind. Eng. Chem. Res*. 2006, *45*, 1945-1954.
[11] Rosenberg, H.S. Byproduct gypsum from flue gas desulfurization processes. *Ind. Eng. Chem. Res.* 1986, *25*, 348-355.
[12] Fan, M.; Brown, R. C.; Zhuang, Y.; Cooper, A. T.; Nomura, M. Reaction kinetics for a novel flue gas cleaning technology. *Environ. Sci. Technol.* 2003, *37*, 1404-1407.
[13] Zeman, F. Energy and material balance of CO_2 capture from ambient air. *Environ. Sci. Technol*. 2007, *41*, 7558-7563.
[14] Scott, K.; Taama, W.; Cheng, H. Towards an electrochemical process for recovering sulphur dioxide. *Chem. Eng. J.* 1999, *73,* 101-111.
[15] Struck, B. D.; Junginger, R.; Boltersdorf, D.; Gehrmann, J. The anodic oxidation of sulfur dioxide in the sulfuric acid hybrid cycle. *Intern. J. Hydrogen Energy*. 1980, *5,* 487-497.
[16] Wiesener, K. The electrochemical oxidation of sulphur dioxide at porous catalysed carbon electrodes in sulphuric acid. *Electrochim. Acta* 1973, *18,* 185-189.
[17] Huang, C.; Xu, T.; Yang, X. Regenerating fuel-gas desulfurizing agents by using bipolar membrane electrodialysis (BMED): effect of molecular structure of alkanolamines on the regeneration performance. *Environ. Sci. Technol.* 2007, *41*, 984-989.
[18] Huang, C.; Xu, T. Electrodialysis with bipolar membranes for sustainable development. *Environ. Sci. Technol*. 2006, *40*, 5233-5243.
[19] Connick, R. E.; Zhang, Y. -X.; Lee, S. Y.; Adamic, R.; Chieng, P. Kinetics and mechanism of the oxidation of HSO_3^- by O_2. 1. the uncatalyzed reaction. *Inorg. Chem.* 1995, *34*, 4543-4553.
[20] Liu, H.; Wang, C.; Li, X.; Xuan, X.; Jiang, C.; Cui, H. A novel electro-Fenton process for water treatment: reaction-controlled pH adjustment and performance assessment. *Environ. Sci. Technol*. 2007, *41*, 2937-2942.
[21] Gözmen, B.; Oturan, M. A.; Oturan, N.; Erbatur, O. Indirect electrochemical treatment of bisphenol in water via electrochemically generated Fenton's reagent. *Environ. Sci. Technol*. 2003, *37*, 3716-3723.
[22] Brillas, E.; Calpe, J. C.; Casado, J. Mineralization of 2,4-D by advanced electrochemical oxidation processes. *Water Res.* 2000, *34*, 2253-2262.
[23] Konnick, R. E.; Zhang, Y.-X. Kinetics and mechanism of the oxidation of HSO_3^- by O_2. 2. the manganese (II)-catalyzed reaction. *Inorg. Chem*. 1996, *35*, 4613-4621.
[24] Vidal, B. F.; Ollero, P.; Gutierrez Ortiz, F. J.; Arjona, R. Catalytic oxidation of S(IV) in seawater slurries of activated carbon. *Environ. Sci. Technol*. 2005, *39*, 5031-5036.
[25] Komintarachat, C.; Trakarnpruk, W. Oxidative desulfurization using polyoxometalates. *Ind. Eng. Chem. Res.* 2006, *45*, 1853-1856.
[26] Yu, G.; Lu, S.; Chen, H.; Zhu, Z. Oxidative desulfurization of diesel fuels with hydrogen peroxide in the presence of activated carbon and formic acid. *Energy & Fuels* 2005, *19*, 447-452.
[27] Streeter, I.; Wain, A. J.; Davis, J.; Compton, R. G. Cathodic reduction of bisulfite and sulfur dioxide in aqueous solutions on copper electrodes: an electrochemical ESR study. *J. Phys. Chem. B* 2005, *109,* 18500-18506.
[28] Trost, B. M. The atom economy-a search for synthetic efficiency. *Science* 1991, *254*, 1471-1477.

[29] Lankey, R. L.; Anastas, P. T. Life-cycle approaches for assessing green chemistry technologies. *Ind. Eng. Chem. Res.* 2002; *41*, 4498-4502.

[30] Wang C., Liu H., Li X.Z., Shi J.Y., Ouyang G.F., Peng M., Jiang C.C., Cui H.N., A new concept of desulfurization: the electrochemically driven and green conversion of SO_2 to $NaHSO_4$ in aqueous solution. Environ. Sci. Technol., 2008, 42, 8585-8590.

INTECH

INTECH



Green Chemistry - Environmentally Benign Approaches
Edited by Dr. Mazaahir Kidwai

ISBN 978-953-51-0334-9
Hard cover, 156 pages
Publisher InTech
Published online 23, March, 2012
Published in print edition March, 2012

Green chemistry is chemistry for the environment. It is really a philosophy and way of thinking that can help chemistry in research and production to develop more eco-friendly solutions. Green chemistry is considered an essential piece of a comprehensive program to protect human health and the environment. In its essence, green chemistry is a science-based non-regulatory and economically driven approach to achieving the goals of environmental protection and sustainable development. Combining the technological progress with environmental safety is one of the key challenges of the millennium. In this context, this book describes the environmentally benign approaches for the industries as well as chemical laboratories. In order to provide an insight into step change technologies, this book was edited by green organic chemists.

How to reference
In order to correctly reference this scholarly work, feel free to copy and paste the following:

Hong Liu, Chuan Wang and Yuan Liu (2012). Electrochemically-Driven and Green Conversion of SO2 to NaHSO4 in Aqueous Solution, Green Chemistry - Environmentally Benign Approaches, Dr. Mazaahir Kidwai (Ed.), ISBN: 978-953-51-0334-9, InTech, Available from: http://www.intechopen.com/books/green-chemistry-environmentally-benign-approaches/electrochemically-driven-and-green-conversion-of-so2-to-nahso4-in-aqueous-solution-

INTECH
open science | open minds

InTech Europe
University Campus STeP Ri
Slavka Krautzeka 83/A
51000 Rijeka, Croatia
Phone: +385 (51) 770 447
Fax: +385 (51) 686 166
www.intechopen.com

InTech China
Unit 405, Office Block, Hotel Equatorial Shanghai
No.65, Yan An Road (West), Shanghai, 200040, China
中国上海市延安西路65号上海国际贵都大饭店办公楼405单元
Phone: +86-21-62489820
Fax: +86-21-62489821